



Article

Association between Proinflammatory Markers, Leukocyte–Endothelium Interactions, and Carotid Intima–Media Thickness in Type 2 Diabetes: Role of Glycemic Control

Aranzazu Martínez de Marañón ¹, Francesca Iannantuoni ¹, Zaida Abad-Jiménez ¹, Francisco Canet ¹, Pedro Díaz-Pozo ¹, Sandra López-Domènech ¹, Ildefonso Roldán-Torres ², Carlos Morillas ¹, Milagros Rocha ^{1,3,*} and Víctor M. Víctor ^{1,3,4,*}

¹ Service of Endocrinology and Nutrition, University Hospital Doctor Peset, Foundation for the Promotion of Health and Biomedical Research in the Valencian Region (FISABIO), 46017 Valencia, Spain; amardema@alumni.uv.es (A.M.d.M.); franian@alumni.uv.es (F.I.); zaiaji@alumni.uv.es (Z.A.-J.); francisco.canet.1994@gmail.com (F.C.); pedrodps2@gmail.com (P.D.-P.); Sandra.Lopez@uv.es (S.L.-D.); carlos.morillas@uv.es (C.M.)

² Service of Cardiology, University Hospital Doctor Peset, Foundation for the Promotion of Health and Biomedical Research in the Valencian Region (FISABIO), 46017 Valencia, Spain; il.roltant@comv.es

³ Centro de Investigación Biomédica en Red (CIBERehd)—Department of Pharmacology, University of Valencia, 46010 Valencia, Spain

⁴ Department of Physiology, University of Valencia, 46010 Valencia, Spain

* Correspondence: milagros.rocha@uv.es (M.R.); victor.victor@uv.es (V.M.V.); Tel.: +34-963189132 (M.R. & V.M.V.)

Received: 4 June 2020; Accepted: 29 July 2020; Published: 5 August 2020



Abstract: Glycated hemoglobin monitorization could be a tool for maintaining type 2 diabetes (T2D) under control and delaying the appearance of cardiovascular events. This cross-sectional study was designed to assess the role of glycemic control in modulating early-stage markers of cardiovascular complications. One hundred and eight healthy controls and 161 type 2 diabetic patients were recruited and distributed according to their glycemic control, setting the threshold at 6.5% (good control). Biochemical and anthropometrical parameters were registered during the initial visit, and peripheral blood was extracted to obtain polymorphonuclear cells and analyze inflammatory markers, adhesion molecules, leukocyte–endothelium interactions, and carotid intima–media thickness. Correlations between these parameters were explored. We found that inflammatory markers and adhesion molecules were augmented in type 2 diabetic subjects with poor glycemic control. Polymorphonuclear leukocytes interacted more with the endothelium in the diabetic population, and even more significantly in the poorly controlled subjects. In parallel, carotid intima–media thickness was also increased in the diabetic population, and the difference was greater among poorly controlled subjects. Finally, correlation measurement revealed that carotid intima–media thickness was related to glycemic control and lipid metabolism in diabetic patients. Our results suggest that glycemic control delays the onset of cardiovascular comorbidities in diabetic subjects.

Keywords: type 2 diabetes; glycated hemoglobin; carotid intima–media thickness; inflammation; endothelial function

1. Introduction

Type 2 diabetes (T2D) is currently one of the most prevalent metabolic diseases, affecting around 500 million people. Its incidence has doubled since 1980 [1,2], increasing health expenditure because

of T2D itself and due to its derived complications [1–4]. In fact, cardiovascular diseases (CVD) are the leading cause of death among type 2 diabetic subjects [2,5], being caused mainly by advanced atherosclerosis, which can be delayed or prevented by early and maintained glycemic control. One of the key markers of glycemic control is glycated hemoglobin (HbA_{1c}), and reducing its levels is a primary goal of diabetic treatment [6–8]. In fact, several studies have demonstrated that sustaining HbA_{1c} below 6.5% reduces the incidence of macro- and microvascular comorbidities [7,9–13].

T2D is associated with a proinflammatory background, caused by high circulating glucose, accumulation of advanced glycation end products (AGEs), glycation of hemoglobin, alteration of lipid metabolism in adipose tissue, and other metabolic alterations that favor a proinflammatory state in peripheral blood [14–16]. If sustained for long periods, all of these modifications promote the production by tissue of a wide array of proinflammatory cytokines such as Interleukin-6 (IL6) and Tumor Necrosis Factor alpha (TNF α), as well as reactive oxygen species (ROS) [15–20], specially by mitochondria. In short, hyperglycemia and hyperlipidemia trigger Nod-Like Receptor Protein NLRP inflammasome activation, TNF α synthesis, and the production of mitochondrial and nonmitochondrial ROS [21–23]. This induces Nuclear Factor Kappa B (NF κ B) activation and inflammatory cytokine expression, mostly through thioredoxin-related protein action [24–27]. Moreover, lipids can react with ROS and amplify the proinflammatory cascade [28]. This results in a vicious cycle of cell death and greater inflammation [29]. This ROS–inflammation axis has been studied in a wide array of inflammatory-based diseases, such as cardiac alterations [30–32], bone and joint diseases [33–35], neuronal and cerebral dysfunctions [28,29,36], bacterial infection [37], liver diseases [38], respiratory alterations [39,40] and cancer [41]. Furthermore, in T2D, the continuous presence of proinflammatory molecules causes diverse endocrine effects on the vasculature, and contributes to the development of micro- and macrovascular pathologies such as carotid atherosclerosis [21]. Together, the sustained increase of ROS production and the rise in inflammation have an important effect on the development of diabetic atherosclerosis [22].

Immune cells are also activated in T2D, producing more proinflammatory and adhesion molecules [15,16,42,43]. As explained previously, circulating proinflammatory molecules produced by chronic hyperglycemia and hyperlipidemia can activate leukocytes and the endothelium [44,45]. In this state, immune cells interact with the endothelium, infiltrating the inner layers of tissues and intensifying the inflammation [15,44,45]. There are different epidemiologic studies describing how an increased leukocyte count is a risk factor for the progression of carotid atherosclerosis and cardiovascular events [46–48]. Proinflammatory factors also favor the development of the atherosclerotic plaque, as demonstrated by several studies [49–52]. In fact, atherosclerosis represents the culmination of continued subclinical inflammation, and is one of the main causes of cardiovascular comorbidities [6,23,53–55]. Worryingly, atherosclerosis is often asymptomatic for decades before clinical manifestations appear, and is termed subclinical atherosclerosis during this period [6,56,57].

Carotid intima–media thickness (CIMT) is a biomarker of subclinical atherosclerosis [58,59]. Measurement of the CIMT by B-mode ultrasound has been shown to be suitable for evaluating the early stages of atherosclerosis [57,60,61] and to be an indicator of CVD [62–64]. Different studies have described a rise of CIMT in T2D [63,65,66] and metabolic syndrome [67,68].

The aim of this study was to explore the potential involvement of glycemic control in inflammation, adhesion molecules, leukocyte–endothelium interactions, and the CIMT in T2D patients compared with a healthy control population.

2. Experimental Section

2.1. Human Subjects

This study was carried out in 269 subjects, specifically, 161 T2D patients and 108 healthy controls recruited from the Service of Endocrinology and Nutrition of University Hospital Doctor Peset (Valencia, Spain) until June 2019 and adjusted for age and sex. The time that these patients had suffered from T2D, the presence of comorbidities, and their drug prescriptions are specified in

Supplementary data (Tables S1–S3). The subjects signed a written informed consent form and protocols were approved by our hospital's Ethics Committee for Clinical Investigation (ID: 98/19), in line with the ethical principles of the Helsinki declaration. T2D patients were diagnosed following the American Diabetes Association (ADA) indications, and presence of morbid obesity, insulin treatment, or any autoimmune, hematological, malignant, infectious, organic, or inflammatory disease represented the exclusion criteria.

2.2. Sample Collection

Venous blood samples were obtained from the antecubital vein in fasting conditions. Weight (kg), height (m), body mass index (BMI; kg/m²), systolic and diastolic blood pressure (SBP/DBP; mmHg), and waist circumference (cm) were assessed previous to the blood extraction.

2.3. Laboratory Tests

Serum was isolated from the blood by centrifugation for 10 min at 1500 g and 4 °C. Fasting glucose, cholesterol, and triglycerides were determined by an enzymatic method. High-density lipoprotein cholesterol (HDL-c) levels were measured with a Beckman LX-20 autoanalyzer (Beckman Coulter, La Brea, CA, USA) using a direct method. Low-density lipoprotein cholesterol (LDL-c) was determined with Friedewald's formula. An immunochemiluminescence assay was employed to determine insulin levels. Homeostatic Model Assessment of insulin resistance HOMA-IR index [fasting insulin (μU/mL) × fasting glucose (mg/dl)/405] was calculated to estimate insulin resistance (IR). Percentage of HbA_{1c} was determined with an automatic glycohemoglobin analyzer (Arkay, Inc., Kyoto, Japan). Apolipoproteins were measured with an electroimmunoassay. High-sensitivity C-reactive protein (hsCRP) was analyzed employing an immunonephelometer (Behring Nephelometer II, Dade Behring, Inc., Newark, DE, USA).

2.4. Leukocyte Isolation

In this assay, polymorphonuclear leukocytes (PMNs) were isolated from heparinized whole blood by the following protocol: the blood was mixed with 1:2 volumes of dextran solution (3% in NaCl 0.9%; Sigma Aldrich, MO, USA) and incubated for 45 min. The supernatant was then poured over Ficoll-Hypaque (GE Healthcare, Uppsala, Sweden) and centrifuged at 650× g for 25 min. The resulting pellet was lysed to remove the remaining erythrocytes with lysis buffer (5 min at room temperature) and centrifuged at 240× g. Pellets containing leukocytes were then washed twice and resuspended in Hank's balanced salt solution (HBSS; Sigma Aldrich, MO, USA). This cellular suspension was employed to perform the leukocyte–endothelium interaction assay.

2.5. Soluble Cytokines and Adhesion Molecule Assay

Intercellular adhesion molecule 1 (ICAM-1), vascular cell adhesion molecule-1 (VCAM-1), P-selectin, IL-6, and TNFα were analyzed in serum samples with a Luminex 200 flow analyzer system (Millipore, Austin, TX, USA). In brief, specific antibodies covered the color-coded microbead, and detection was performed with biotinylated secondary antibody and streptavidin-PE conjugate. The fluorescence of each individual microbead was analyzed with the Luminex XMap instrument. This method allows multiple cytokines in the same sample to be analyzed with a high specificity and sensitivity. The TNFα detection range was between 1750 and 0.43 pg/mL; that of IL-6 is 750 to 0.18 pg/mL; that of VCAM-1 is 500 to 0.122 ng/mL; that of ICAM-1 is 350 to 0.085 ng/mL; and that of P-selectin is 1000 to 0.122 ng/mL. The intra-assay %CV is <5% for TNFα and IL-6 and <15% for ICAM-1, VCAM-1, and P-selectin. The interassay %CV is <20% for IL-6, ICAM-1, VCAM-1, and P-selectin and <15% for TNFα.

2.6. Static Cytometry Measurements

Mitochondrial ROS production was evaluated employing a MitoSOX (Thermo Fisher Scientific, Waltham, MA, USA) fluorescent probe. A fluorescence microscope (IX81; Olympus Corporation, Shinjuku-ku, Tokyo, Japan) with automated static cytometry software (ScanR, Olympus, Munich, Germany), which measures the fluorescence emission per individual cell, was also used. In brief, the protocol consisted of seeding PMN, extracted as previously specified, in 48-well plates and allowing them to adhere to the well surface. MitoSOX and DAPI (Sigma Aldrich, MO, USA) were then added to the well at a final concentration of 0.1 μ M, for 20 min. After washing the cells twice with HBSS, fluorescence was measured and MitoSOX emission data relativized to DAPI emission data for each cell. PMN data were relativized with an internal control for all the experiments. All experiments were performed in duplicate, and 16 images per well were measured.

2.7. PMN–Endothelium Interaction Assay

An aliquot of 1.2 mL PMNs, isolated as previously described [69], with a density of 10^6 cells/mL in complete Roswell Park Memorial Institute medium RPMI, was employed for this assay. Primary cultures of human umbilical cord endothelial cells (HUVEC) were prepared as reported in [69]. In this assay, the PMN aliquot was perfused across the endothelial monolayer at a speed of 0.3 mL/min over a 5 min period, and the process was recorded. Rolling PMNs were considered to be those rolling for at least 1 min. Velocity was assessed by determining the time in which 15 rolling PMNs covered a distance of 100 μ m. Adhesion was analyzed by counting the number of PMNs adhering to the endothelium for at least 30 s in 5 different fields.

2.8. Assessment of Carotid Intima–Media Thickness (CIMT)

Carotid thickness was evaluated following the American Echocardiography Association's guidelines. Healthy subjects and T2D patients were told to attend the Cardiology Service of the Dr. Peset Hospital 7–10 days after the blood extraction in order to evaluate carotid intima–media thickness. This measure has a diagnostic value because of its positive correlation with risk factors and with the prevalence of cardiovascular and cerebrovascular disease. The evaluation was performed by placing the head of the patients at 45° with respect to the body longitudinal axis. Some subjects were dropped from the study due to clinical or schedule reasons.

Carotid sonography was performed with a single ultrasound machine Aloka 5500 (Hitachi Aloka, Tokyo, Japan) equipped with a 7.5 MHz sector scanner probe. Baseline and follow-up studies were performed in a standard fashion by a single specialist physician who was specifically trained to perform the examination and was blinded to the treatment group. All images were electronically stored. Measurements corresponded with the 1 cm segment proximal to the dilation of the carotid bulb, and were always performed in plaque-free segments. For each patient, three measurements were performed for both sides of the anterior, lateral, and posterior projections of the far wall, and readings were then averaged. An independent observer, who was blinded to the treatment group and trained to interpret the CIMT images, performed an off-line analysis of B-mode ultrasound images. Paired CIMT measurements in the same arteries showed a high degree of reproducibility, with a mean difference in CIMT of 0.020 mm, and an intraclass correlation coefficient of 0.97 ($p < 0.001$). CIMT regression was defined as a decrease of >0.020 mm in mean CIMT at 12 months.

2.9. Statistical Analysis

All data were analyzed with SPSS 17.0 software (SPSS Statistics Inc., Chicago, IL, USA). Values are expressed as mean and standard deviation (SD) for parametric data, while the median (25th–75th percentiles) is presented for nonparametric data. Bar graphs show mean and standard error of the mean (SEM) in the figures. Multivariate lineal analysis was performed to check the influence of BMI and age on the other dependent variables.

Correlation analysis was performed with the Spearman formula, and the linear regression coefficient was also calculated. Graphs were plotted with GraphPad Prism 4.0 (GraphPad, La Jolla, CA, USA).

Multivariate linear analysis was performed in order to eliminate the influence of BMI and age on the variables of interest. Normality of the data sets was assessed by Kolmogorov–Smirnov test. In the case of the variables with normally distributed data, the groups were compared with a Student's *t*-test, while a Mann–Whitney U test was employed for non-normally distributed ones, and the Chi-Square test for proportion of frequencies. Study groups were compared using one-way analysis of variance (ANOVA) followed by a Bonferroni post hoc test. Differences were considered to be significant when $p < 0.05$, applying a confidence interval of 95% in every comparison. Graphs were plotted with GraphPad Prism 4.0 (GraphPad, La Jolla, CA, USA).

3. Results

3.1. Anthropometric and Biochemical Parameters

The study population was initially divided into healthy controls (108) and T2D patients (161) following the diagnostic criteria of the ADA. Diabetic patients were divided into two populations depending on their glycemic control, which was represented by their levels of HbA_{1c}. The set threshold was 6.5, in line with ADA criteria [7]. Table 1 confirms that both diabetic populations had typical hallmarks, with significant differences in glucose ($p < 0.01$), HbA_{1c} ($p < 0.01$), and HOMA index ($p < 0.01$). Moreover, significant differences in glucose levels ($p < 0.001$) and HOMA index ($p < 0.001$) were found between the T2D HbA_{1c} > 6.5 group and the T2D HbA_{1c} ≤ 6.5 group. Our T2D populations also displayed features such as greater waist diameter ($p < 0.01$), increased waist-to-hip ratio ($p < 0.01$), higher HOMA index ($p < 0.01$), and altered lipid metabolism parameters, with increased VLDL and triglyceride levels ($p < 0.01$), Ct/HDL ($p < 0.01$), and AIP ($p < 0.01$) and lower levels of HDL-c ($p < 0.01$). Total cholesterol, LDL cholesterol, and non-HDL cholesterol levels remained unchanged in the T2D HbA_{1c} ≤ 6.5% group. However, total and LDL cholesterol were significantly reduced ($p < 0.01$) in the T2D HbA_{1c} > 6.5 group, possibly due to the hypolipemiant treatment. Regarding apolipoproteins, ApoA1 was significantly lower in T2D patients with respect to healthy controls ($p < 0.01$) and the difference was even more significant in the HbA_{1c} > 6.5% group ($p < 0.001$). ApoB levels did not change. Interestingly, the ApoB/ApoA ratio significantly increased in the T2D HbA_{1c} > 6.5 population ($p < 0.01$).

3.2. Inflammation Markers

A hyperglycemic scenario is usually accompanied by an increase in subclinical inflammation levels. We analyzed some relevant proinflammatory markers in our cohort of patients and their respective controls. The T2D group showed a significant increase in TNFα levels compared to the control group ($p = 0.047$) (Figure 1A). When we distributed the T2D population based on HbA_{1c}, an increase was preserved in the T2D HbA_{1c} > 6.5 group ($p = 0.014$) (Figure 1B). Another relevant cytokine, IL-6, was doubled in T2D subjects ($p = 0.019$) (Figure 1C) and, as occurred with TNFα, the increase was associated with T2D HbA_{1c} > 6.5% ($p = 0.015$) (Figure 1D).

Moreover, we evaluated mtROS production, and the results showed a significant rise in mtROS in the T2D population ($p = 0.045$) (Figure 1E), which was more pronounced among the poorly controlled population ($p = 0.038$) (Figure 1F). Poorly controlled T2D patients also had significantly higher levels of mtROS than their well-controlled counterparts ($p = 0.041$) (Figure 1F).

3.3. PMN–Endothelium Interactions

The generalized state of inflammation during T2D entails the activation of immune cells, which, in an active state, are more prone to attach to the endothelium and infiltrate through to the inner layers of the organs. Thus, we analyzed serum levels of adhesion molecules such as ICAM-1, VCAM-1,

and P-selectin, some of the main players of leukocyte–endothelium interactions. As can be seen in Figure 2, T2D patients displayed higher levels of ICAM-1 ($p = 0.016$) (Figure 2A) and VCAM-1 ($p = 0.027$) (Figure 2C), but not of P-selectin. The increase in ICAM-1 was already significant in the well-controlled diabetic population ($p = 0.006$) (Figure 2B), and was enhanced in the poorly controlled diabetic population ($p < 0.001$). In addition, VCAM-1 was significantly higher in T2D subjects with $HbA_{1c} > 6.5\%$ ($p = 0.005$) (Figure 2D).

Table 1. Anthropometrical and biochemical parameters.

	Control	T2D	
		$HbA_{1c} \leq 6.5\%$	$HbA_{1c} > 6.5\%$
N	108	57	104
Age (Years)	57 ± 11	58 ± 8	60 ± 9
%Women	62.2%	43.93%	56.11%
Weight (kg)	68.51 ± 15.18	85.02 ± 16.07 *	83.59 ± 15.84 *
BMI (kg/cm ²)	24.18 ± 4.11	31.18 ± 4.23 *	30.43 ± 5.13 *
SBP (mmHg)	119.43 ± 18.18	139.82 ± 14.23 *	138.38 ± 17.05 *
DBP (mmHg)	72.35 ± 10.94	82.03 ± 10.97 *	78.25 ± 9.35 *
Waist (cm)	79.81 ± 12.62	106.39 ± 11.46 *	103.99 ± 13.35 *
Hip (cm)	99.09 ± 7.21	108.71 ± 9.53 *	108.48 ± 12.62 *
Waist–Hip ratio	0.80 ± 0.09	0.97 ± 0.08 *	0.95 ± 0.08 *
Glucose (mg/dL)	88.08 ± 10.75	112.37 ± 22.59 *	160.51 ± 55.06 *‡
HOMA	1.69 ± 1.19	3.72 ± 2.00 *	6.57 ± 4.45 *‡
HbA _{1c} (%)	5.18 ± 0.26	5.94 ± 0.30 *	7.85 ± 1.30 *
Total cholesterol (mg/dL)	185.43 ± 35.32	173.67 ± 34.31	167.42 ± 37.67 *
HDL-c (mg/dL)	56.04 ± 13.61	45.10 ± 11.83 *	42.94 ± 10.46 *
LDL-c (mg/dL)	111.38 ± 28.72	102.62 ± 31.33	95.17 ± 31.09 *
VLDL (mg/dL)	26.01 ± 10.81	28.63 ± 19.54 *	28.91 ± 22.04 *
Cholesterol/HDL	3.46 ± 0.94	4.07 ± 1.18 *	4.06 ± 1.14 *
Triglycerides (mg/dL)	87.62 (55.50; 103.00)	130.29 (90.5; 169.00) *	150.75 (92.00; 162.63) *
Non-HDL Cholesterol (mg/dL)	129.39 ± 33.28	129.37 ± 32.51	124.48 ± 36.57
AIP (TG/HDL-c)	0.10 (−0.06; 0.33)	0.47 (0.23; 0.63) *	0.47 (0.29; 0.68) *
APO A1 (mg/dL)	164.02 ± 32.28	151.45 ± 27.21 *	142.72 ± 22.87 *‡
APO B (mg/dL)	90.78 ± 26.60	90.33 ± 25.82	94.18 ± 25.27
APOB/APOA1	0.57 ± 0.20	0.64 ± 0.24	0.67 ± 0.19 *
hsCRP (mg/L)	0.75 (0.36; 1.83)	2.64 (1.61; 7.07) †	2.87 (1.31; 6.59) †

Anthropometrical and biochemical parameters obtained from whole peripheral blood from healthy subjects, $HbA_{1c} \leq 6.5\%$ T2D patients and $HbA_{1c} > 6.5\%$ T2D patients after 12 h fasting. Kolmogorov–Smirnov normality test was performed in all data sets. Data are shown as mean ± SD for data with normal distribution, and median and 25th; 75th percentile for non-normal data. The differences were analyzed by a t-test in the case of normal data and a Mann–Whitney test in that of non-normal data. *, $p < 0.01$ vs. control; †, $p < 0.001$ vs. control; ‡, $p < 0.001$ vs. T2D $HbA_{1c} \leq 6.5\%$.

For assessing PMN–endothelium cell interactions directly, we performed an in vitro adhesion assay with leukocytes from T2D patients and their respective controls. Leukocyte count was slightly higher but within the normal range in T2D patients. This could reflect the subclinical inflammation level characteristic of T2D (Supplementary Table S4). Rolling number, rolling velocity, and adhesion to the endothelial monolayer were assessed. We obtained a higher number of rolling cells in T2D patients ($p < 0.001$) (Figure 2G), accompanied by a lower velocity of these cells ($p < 0.001$) (Figure 2I) and a higher level of adhesion to the endothelial monolayer ($p < 0.001$) (Figure 2K). These differences remained when we separated the T2D population depending on its glycemic control status ($p < 0.001$) (Figure 2H,J,L). PMN rolling ($p < 0.001$) and adhesion ($p < 0.05$) were increased, while rolling velocity was decreased ($p < 0.001$) in well-controlled diabetic subjects. These significant differences were sustained in poorly controlled diabetic subjects, and were more significant in the case of cell adhesion (p

< 0.001). These differences can be assessed in the Supplementary Videos (Supplementary Videos S1–S3), in which representative videos of each experimental group have been attached (Supplementary data).

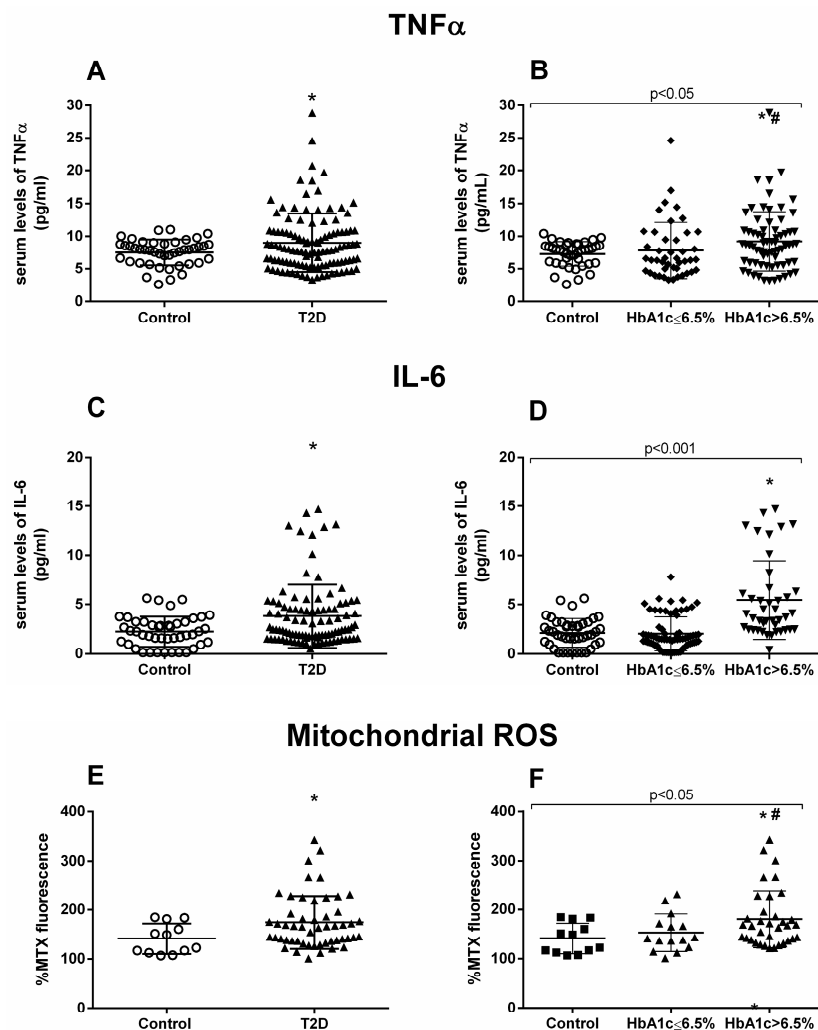


Figure 1. TNF α , IL-6, and mtROS measurements. Serum levels of proinflammatory cytokines TNF α (A,B) and IL-6 (C,D), and fluorescence levels of mtROS (E,F). Differences between control and T2D groups (A,C,E) or between control, well-controlled (HbA_{1c} ≤ 6.5%) and poorly controlled diabetic groups (HbA_{1c} > 6.5%) (B,D,F) are shown. Statistical analysis was performed using a t-test to compare two groups, and using ANOVA with Bonferroni post-test for three groups. * $p < 0.05$ vs. control; # $p < 0.05$ vs. T2D HbA_{1c} < 6.5%.

3.4. Carotid Intima–Media Thickness Measurements

The proinflammatory environment seen in our diabetic patients and the increase in leukocyte–endothelium interactions could represent a rise in the incidence of macro- and microvascular complications. Therefore, we next explored CIMT. All the patients underwent carotid echocardiography at our hospital’s Cardiology Service. Diabetic patients showed higher CIMT compared to healthy controls, with this difference being identified in the left carotid ($p < 0.001$) (Figure 3A) and right carotid ($p = 0.003$) (Figure 3C).

We observed that the poorly controlled diabetic population had significantly higher left CIMT than the well-controlled diabetic group ($p = 0.024$) (Figure 3B). On the other hand, right CIMT proved to be significantly higher in the poorly controlled diabetic group than in the control group ($p = 0.001$) (Figure 3D).

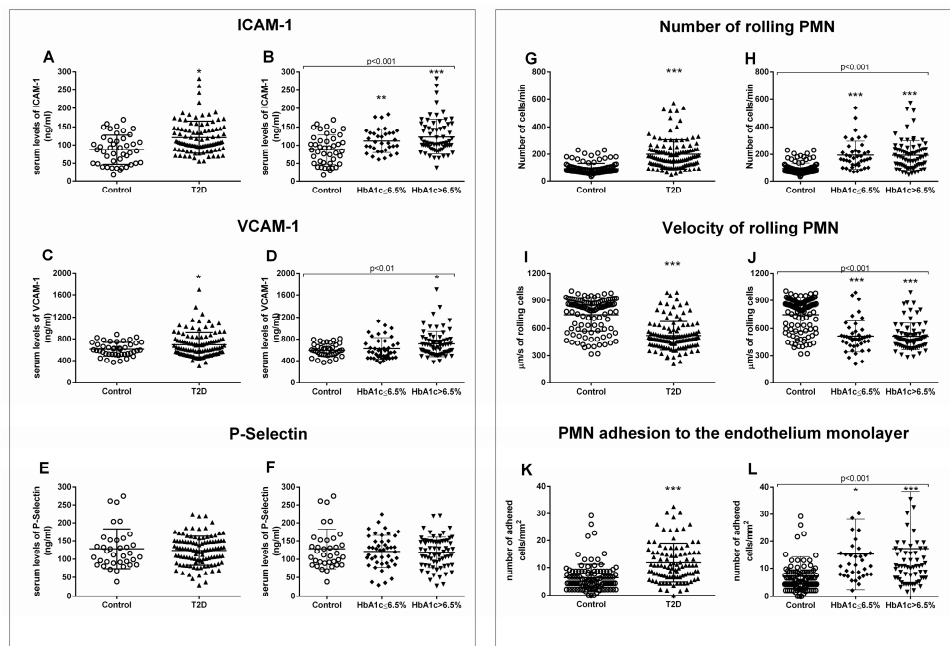


Figure 2. Serum levels of soluble adhesion molecules and measurement of PMN–endothelium interactions. Differences in adhesion molecules between control and T2D groups (A,C,E) or between control, well-controlled diabetics ($HbA_{1c} \leq 6.5\%$), and poorly controlled diabetics ($HbA_{1c} > 6.5\%$) (B,D,F) are shown. The number of rolling cells (G,H), their velocity (I,J), and the adhesion of these cells to the endothelial monolayer (K,L) were analyzed. Differences between control and T2D groups (G,I,K) or between control, well-controlled diabetics ($HbA_{1c} \leq 6.5\%$), and poorly controlled diabetic groups ($HbA_{1c} > 6.5\%$) (H,J,L) are shown. Statistical analysis was performed by means of a *t*-test to compare two groups, and using ANOVA with Bonferroni post-test for three groups. * $p < 0.05$; ** $p < 0.01$; *** $p < 0.001$ vs. control.

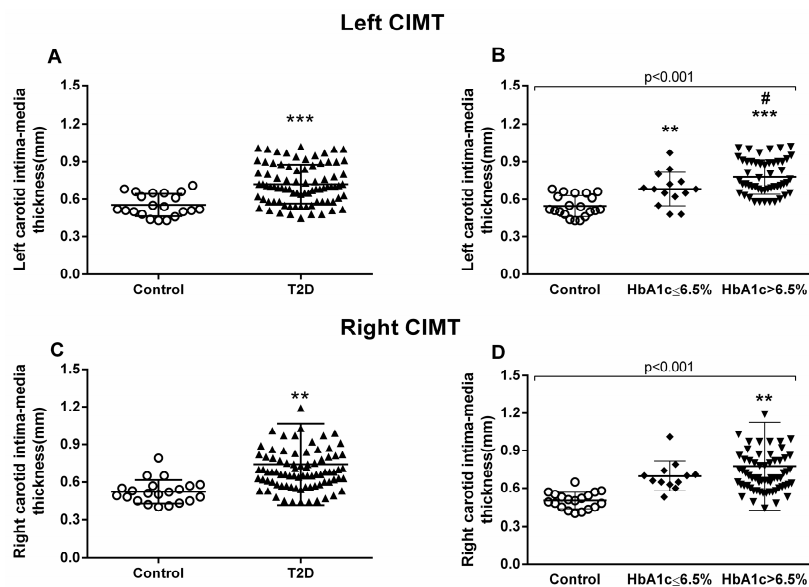


Figure 3. Measurement of carotid intima–media thickness (CIMT). Left carotid (A,B) and right carotid (C,D) were analyzed. Differences between control and T2D groups (A,C) or between control, well-controlled ($HbA_{1c} \leq 6.5\%$), and poorly controlled diabetic groups ($HbA_{1c} > 6.5\%$) (B,D) are shown in the graphs. Statistical analysis was performed by means of a *t*-test to compare two groups, and using ANOVA with a Bonferroni post-test for three groups. ** $p < 0.01$; *** $p < 0.001$ vs. control group; # $p < 0.05$ vs $HbA_{1c} \leq 6.5\%$ group.

3.5. Correlation Analysis

We took all these data and performed correlations and linear regression to explore relations between all the analyzed variables. First, we analyzed the relationship between in vitro adhesion assay parameters and the left CIMT; we observed positive correlations (rolling number Figure 4A, $p = 0.037$, $r = 0.218$; rolling velocity Figure 4C, $p = 0.021$, $r = 0.252$; adhesion Figure 4E, $p = 0.037$, $r = 0.239$) among the left carotid measures but not among those of the right (Figure 4B,D,F).

Regarding biochemical parameters, we saw that left CIMT measures correlated significantly with glucose ($p = 0.003$, $r = 0.203$) (Figure 5A), HOMA-IR ($p < 0.001$, $r = 0.338$) (Figure 5C), BMI ($p = 0.036$, $r = 0.235$) (Figure 5E), and HbA1c ($p < 0.001$, $r = 0.399$) (Figure 5G). These correlations were similar for the right CIMT, except for BMI correlation, which was not significant (Figure 5B (Glucose), $p < 0.001$, $r = 0.377$; Figure 5D (HOMA-IR), $p < 0.001$, $r = 0.360$; Figure 5F (HbA1c), $p < 0.001$, $r = 0.389$).

When we analyzed the correlation with lipid parameters, we observed that left CIMT was significantly correlated with HDL-c ($p < 0.001$, $r = -0.436$) (Figure 6A), VLDL ($p = 0.001$, $r = 0.313$) (Figure 6C), cholesterol/HDL index ($p = 0.001$, $r = 0.313$) (Figure 6E), and AIP ($p = 0.001$, $r = 0.402$) (Figure 6G). The data for right CIMT revealed similar correlations (Figure 6B (HDL-c), $p = 0.025$, $r = -0.222$; Figure 6D (VLDL), $p = 0.007$, $r = 0.270$; Figure 6H (AIP), $p = 0.002$, $r = 0.307$), with the exception of cholesterol/HDL index correlation.

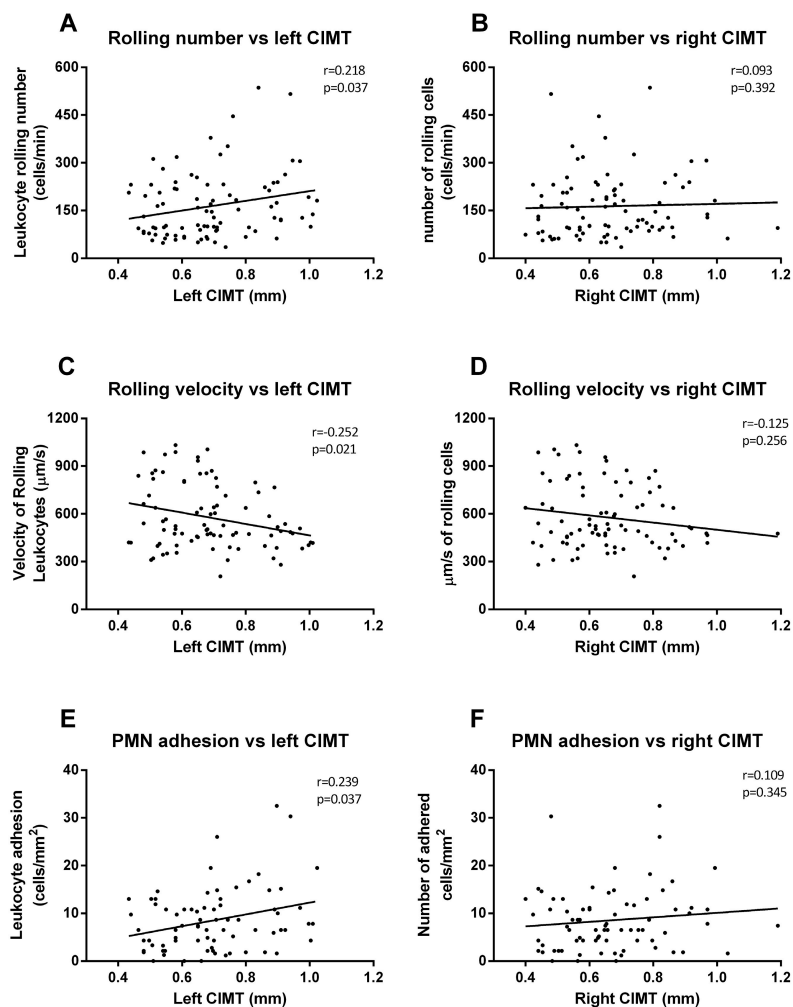


Figure 4. Correlation graphs of adhesion assay vs. CIMT measures. Graphs show correlations between number of rolling PMN and left (A) and right CIMT (B); rolling velocity and left (C) and right CIMT (D); and cell adhesion and left (E) and right CIMT (F). Spearman correlation analysis was performed.

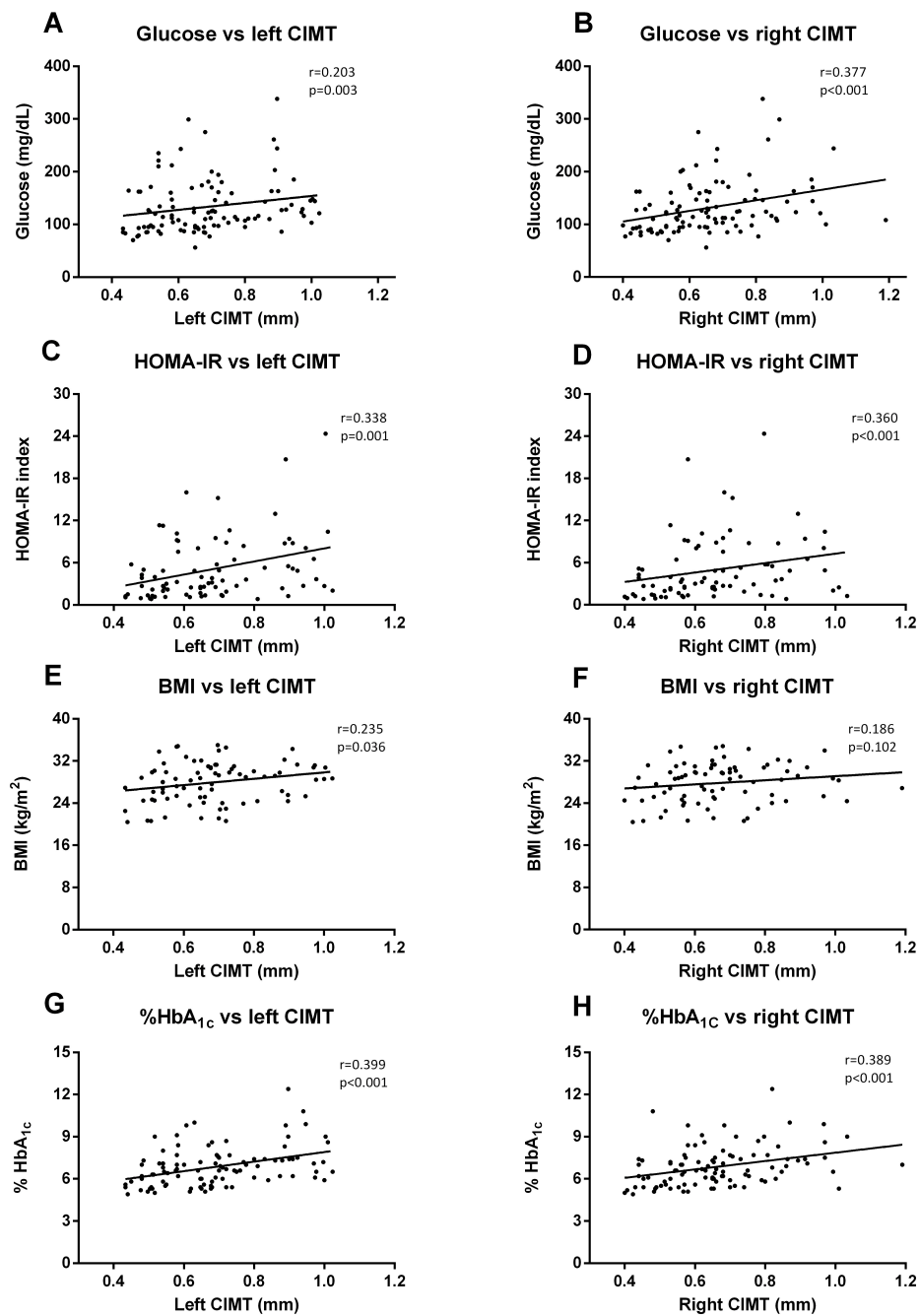


Figure 5. Correlation graphs of biochemical and anthropometrical parameters vs. CIMT measures. Graphs show correlation between glucose levels and left (A) and right CIMT (B); HOMA index and left (C) and right CIMT (D); BMI and left (E) and right CIMT (F); and HbA_{1c} and left (G) and right (H) CIMT. Spearman correlation analysis was performed.

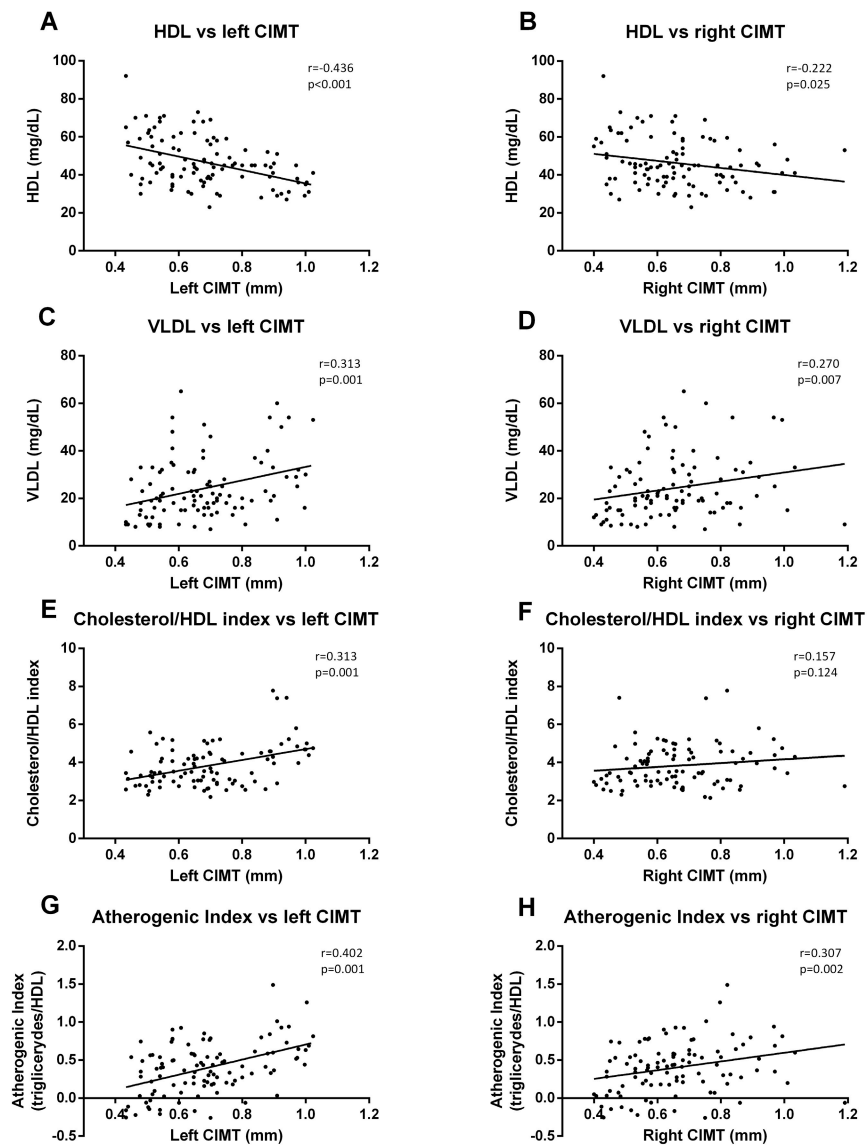


Figure 6. Correlation graphs of lipid metabolism parameters vs. CIMT measurements. Graphs show a correlation of HDL-c with left (A) and right CIMT (B); of VLDL index with left (C) and right CIMT (D); of cholesterol/HDL-c index with left (E) and right CIMT (F); and of atherogenic index (AIP) with left (G) and right (H) CIMT. A Spearman correlation analysis was performed. r coefficient and statistical significance, if any existed, are shown in the graph.

4. Discussion

Cardiovascular complications are a principal concern during diabetes management. The present study gives relevance to the relationship between CIMT, HbA_{1c}, and different hallmarks of T2D (inflammation, ROS production, and leukocyte–endothelium interactions). We have evaluated the involvement of glycemic control in endocrine and anthropometric parameters, inflammatory markers (TNF- α , IL-6, and mtROS production), adhesion molecules (ICAM-1, VCAM-1, and P-selectin), leukocyte–endothelium interactions (rolling, rolling velocity, and adhesion) and CIMT in T2D. In addition, we have analyzed their interrelationship by performing correlation studies. T2D patients, and especially those with poor glycemic control (HbA_{1c} > 6.5%), expressed an increase in inflammatory markers, mtROS production, adhesion molecules, leukocyte–endothelium interactions, and CIMT.

Regarding inflammatory intermediates, our study shows a slight but significant increase in TNF- α and IL-6 production in T2D patients; it is possible that the difference is not bigger because of the

hypolipemiant treatments received by most of the T2D patients. These proinflammatory cytokines are involved in the development of inflammation in T2D. Enhanced levels of TNF- α from leukocytes after activation by ROS-induced oxidative stress are thought to impair glucose uptake and inhibit insulin signaling [70,71]. Furthermore, IL-6 is thought to play an important role in atherosclerosis in T2D [56]. We show an increase in mtROS production in leukocytes from T2D patients that was more pronounced in subjects with HbA_{1c} > 6.5%, suggesting that leukocyte mitochondrial function can be altered during chronic hyperglycemia [70,72–74]. Other studies in the field have suggested that good glycemic control reduces ROS production [57,75,76]. These results are in accordance with those of other studies that have demonstrated high mtROS production in T2D related to the development of silent myocardial ischemia [72]. In this sense, it is important to underline that leukocytes are especially linked to ROS generation and cells that are highly sensitive to the oxidative damage mediated by ROS [77,78].

Different pathophysiological processes, including hypertension and atherosclerosis, are characterized by leukocyte recruitment to the arterial wall. In the present study, we have used an *in vitro* model in which human leukocytes flow over a monolayer of human endothelial cells with a shear stress similar to that observed *in vivo* [72]. This mimics the process that precedes inflammation *in vivo* (rolling and adhesion), and which is critical to homeostasis and vascular cell integrity. Our experimental system has been widely applied to visualize and analyze the multistep recruitment of leukocytes in these diseases, and allows the mechanisms of action implicated in this recruitment to be assessed [79]. Regarding this idea, it has been demonstrated that an inflammatory background favors the increase of leukocyte–endothelium interaction and promotes the early development of atherosclerotic events [80,81]. In the current study, we have observed that T2D enhanced rolling flux and PMN adhesion and reduced the rolling velocity of PMN. These effects were more evident in the group with HbA_{1c} > 6.5%. Furthermore, several studies have demonstrated the importance of leukocytes in the atherosclerotic scenario [82–84]. In accordance with these results, an increase in leukocyte–endothelium interactions has been related to oxidative stress in a human model of insulin resistance [85]. In addition, Petterson et al. demonstrated that there is increased recruitment but impaired function of leukocytes during inflammation in mouse models of T1D and T2D [86].

Endothelial and immune cell activation can be evaluated by measuring the soluble adhesion molecules VCAM-1, ICAM-1, and P-selectin. In this sense, it has been described that adhesion molecules are enhanced in patients with T2D [87]. In the present study, we show an increase in adhesion molecules, ICAM-1 and VCAM-1, in T2D that was most pronounced in the case of VCAM-1 in the HbA_{1c} > 6.5% group. These results are compatible with a rise in the number of leukocyte–endothelium interactions, and it has been demonstrated that hyperglycemia in both normal subjects and T2D patients can induce vasoconstriction, adhesion molecules, and inflammation [88,89]. Importantly, there was a slight but significant increase of T2D adhesion molecule levels with respect to the control group, a difference that may have been reduced by the hypolipemiant treatment.

The measurement of CIMT is useful for monitoring the early stages of atherosclerosis [61,90], and CIMT enhancement has been described in T2D [91]. In the present study, we have observed an increase in left and right CIMT, especially in the former case. Furthermore, the increment was more evident in the HbA_{1c} > 6.5% group, suggesting that glycemic control is crucial for leukocyte–endothelium interactions and, therefore, for CIMT. The relevance of these changes in the left CIMT remain to be clarified, though different studies have suggested variations between left and right carotids; for example, Lorentz M. W. et al. revealed that left carotid plaques were vulnerable, whereas right carotid ones were calcified and stable [65]. Luo X et al. studied the factors associated with left and right CIMT and found that changes in biochemical parameters were associated with left carotid measures, while hemodynamic parameters were more related to right carotid measures [92]. The main consequences of CIMT thickening are cerebrovascular events such as stroke, and left carotid stroke is more frequent because of a higher probability of thickening of the left carotid arterial wall [93,94]. The above mentioned authors highlighted that the location of the left carotid renders it more susceptible to hemodynamic stress, thus increasing the probability of arterial wall thickening and

rupture. Selwaness M. et al. support this hypothesis; they found that while bilateral plaques were more frequent, 67% of cases of unilateral plaque occurred in the left carotid. This left plaque presented more intraplaque hemorrhage and more fibrous tissue and was thicker than the right, all of which explain why the left plaque is more vulnerable and prone to stroke. In the same study, right CIMT was found to be more calcified than the left, which would make it more resistant to shear stress [95].

In the present study, we have observed positive correlations between in vitro adhesion assay parameters and left CIMT, but not right CIMT. These results confirm the relevance of the enhancement of leukocyte–endothelium interactions in CIMT, especially on the left side. In terms of biochemical parameters, left CIMT measures correlated significantly with glucose, HOMA-IR, BMI, and HbA_{1c}. These correlations were maintained in the right CIMT, except for BMI (which was not significant). In line with these results, a systematic review by Einarson et al. found that individuals with impaired glucose tolerance had slightly (though significantly) higher CIMT values than individuals with normal glucose tolerance [96]. This data, together with leukocyte–endothelium interactions, suggest that poor glycemic control leaves T2D diabetic patients more prone to developing early or subclinical atherosclerotic events due to the rise in the number of leukocytes infiltrating the intima–media layer.

Finally, we analyzed correlations between CIMT and lipid parameters, and observed that the left CIMT was significantly correlated with VLDL, cholesterol/HDL index, and AIP. All these correlations were maintained when we analyzed the right CIMT data, with the exception of the cholesterol/HDL index correlation. In this sense, [97] demonstrated that lipid parameters, including total cholesterol (TC), triglycerides (TG), LDL, and VLDL, were significantly higher in diabetic stroke patients and positively correlated with the risk of stroke. CIMT was significantly higher in diabetic stroke patients, and correlations of lipid parameters (TC, TG, and VLDL) with CIMT in said patients were significantly and positively correlated, while lipid parameters (TC, TG, HDL, and LDL) were negatively correlated in nondiabetic ischemic stroke patients. Although lipidic parameters were differently affected by glycemic control, it is clear that these parameters increase the risk of developing later cardiovascular complications by increasing CIMT. We did not find any significant correlation with mitochondrial ROS production, adhesion molecules, or cytokine concentrations, though there was a tendency toward a slight correlation.

This study is observational, and so it would be interesting to perform a longitudinal intervention study in which we assess the evolution of CIMT in patients with poor glycemic control that achieve a good glycemic control. Defining the reason why left and right carotids behave and are affected differently is still unclear, and further research focusing on this issue would be useful. Moreover, we have correlated many T2D markers with one indicator of cardiovascular risk; future studies could attempt to find a correlation with other cardiac and endothelium function markers to reinforce our findings.

5. Conclusions

The current study provides evidence of proinflammatory markers, mtROS production, leukocyte–endothelium interactions, adhesion molecules, and CIMT in T2D. Some of these alterations were more pronounced in patients with HbA_{1c} > 6.5, suggesting that glycemic control is a useful tool for preventing or delaying the onset of subclinical atherosclerotic process. Future research into these aspects will help to clarify the molecular mechanisms involved in glycemic control in T2D, and to modulate and control the atherosclerotic process in T2D.

Supplementary Materials: The following are available online at <http://www.mdpi.com/2077-0383/9/8/2522/s1>, Table S1: Time of T2D evolution on the recruited patients, Table S2: Incidence of most common comorbidities in the recruited T2D patients and in the control population, Table S3: Prescription of the different treatments associated with T2D in all the study subjects, Table S4: Leukocyte composition in healthy subjects and diabetic patients., Video S1: Control, Video S2: HbA_{1c} > 6.5, Video S3: HbA_{1c} ≤ 6.5.

Author Contributions: Conceptualization: V.M.V. and M.R.; Methodology, A.M.d.M., Z.A.-J., F.C., P.D.-P., S.L.-D.; Resources: I.R.-T., C.M., V.M.V., M.R.; Data curation: A.M.d.M., F.I., F.C., V.M.V.; Writing—Original Draft: A.M.d.M. and F.I.; Writing—Review and Editing: V.M.V., S.L.-D., and M.R.; Visualization: A.M.d.M. and F.I.

Supervision: C.M., V.M.V. and M.R.; Project administration: V.M.V., I.R.-T., M.R.; Funding acquisition: V.M.V., M.R. All authors have read and agreed to the published version of the manuscript.

Funding: This study was financed by grants PI19/00838, PI19/0437, and CIBERehd CB06/04/0071 by Carlos III Health Institute and by the European Regional Development Fund (ERDF “A way to build Europe”); UGP-15-220 by FISABIO; PROMETEO/2019/027 by Ministry of Health of the Valencian Regional Government; and by an unrestricted grant from Menarini S.A. A.M. and Z. A.-J. are recipients of PFIS contracts from Carlos III Health Institute (FI17/00126 and FI17/00144, respectively). F.C. is recipient of a Santiago Grisolia contract from the Valencian Regional Government (GRISOLIAP/2019/091). V.M.V. is recipient of CES/10/030 contract and R.M. is recipient of CPII16/00037 contract, both from the Ministry of Health of the Valencian Regional Government and Carlos III Health Institute.

Acknowledgments: The authors thank Brian Normanly (University of Valencia/CIBERehd) for his editorial assistance; and Rosa Falcón for her technical assistance.

Conflicts of Interest: The authors declare no conflict of interest.

Abbreviations

ADA	American Diabetes Association
AGE	Advanced glycation end products
AIP	Atherogenic index of plasma
CIMT	Carotid intima–media thickness
CT	Cholesterol
DAPI	4′6′Diamidin-2-fenilindol
DBP	Diastolic blood pressure
HbA _{1c}	Glycated hemoglobin
HBSS	Hanks’ Balanced Salt Solution
HDLc	High-density lipoprotein cholesterol
HOMA-IR	Homeostatic model assessment–insulin resistance
HUVEC	Human umbilical cord vein endothelial cell
ICAM-1	Intercellular adhesion molecule 1
IL-6	Interleukin 6
IR	Insulin resistance
LDLc	Low-density lipoprotein cholesterol
PMN	Polymorphonuclear cells
ROS	Radical oxygen species
RPMI	Roswell Park Memorial Institute culture medium
SBP	Systolic blood pressure
TG	Triglycerides
TNF α	Tumor necrosis factor alpha
VCAM-1	Vascular cell adhesion molecule 1
VLDLc	Very low-density lipoprotein cholesterol

References

1. NCD Risk Factor Collaboration (NCD-RisC). Worldwide trends in diabetes since 1980: A pooled analysis of 751 population-based studies with 4.4 million participants. *Lancet* **2016**, *387*, 1513–1530. [[CrossRef](#)]
2. Zheng, Y.; Ley, S.H.; Hu, F.B. Global aetiology and epidemiology of type 2 diabetes mellitus and its complications. *Nat. Rev. Endocrinol.* **2018**, *14*, 88–98. [[CrossRef](#)]
3. Zhang, Y.-B.; Pan, X.-F.; Chen, J.; Xia, L.; Cao, A.; Zhang, Y.; Wang, J.; Li, H.; Yang, K.; Guo, K.; et al. Combined lifestyle factors and risk of incident type 2 diabetes and prognosis among individuals with type 2 diabetes: A systematic review and meta-analysis of prospective cohort studies. *Diabetologia* **2020**, *63*, 21–33. [[CrossRef](#)]
4. Stirban, A.O.; Tschöpe, D. Cardiovascular complications in diabetes: Targets and interventions. *Diabetes Care* **2008**, *31* (Suppl. 2), S215–S221. [[CrossRef](#)]
5. Ley, S.H.; Hamdy, O.; Mohan, V.; Hu, F.B. Prevention and Management of Type 2 Diabetes: Dietary Components and Nutritional Strategies. *Lancet* **2014**, *383*, 1999–2007. [[CrossRef](#)]

6. Cosentino, F.; Grant, P.J.; Aboyans, V.; Bailey, C.J.; Ceriello, A.; Delgado, V.; Federici, M.; Filippatos, G.; E Grobbee, D.; Hansen, T.B.; et al. 2019 ESC Guidelines on diabetes, pre-diabetes, and cardiovascular diseases developed in collaboration with the EASD. *Eur. Heart J.* **2020**, *41*, 255–323. [\[CrossRef\]](#)
7. American Diabetes Association. 6. Glycemic Targets: Standards of Medical Care in Diabetes—2018. *Diabetes Care* **2018**, *41* (Suppl. 1), S55–S64. [\[CrossRef\]](#)
8. Laiteerapong, N.; A Ham, S.; Gao, Y.; Moffet, H.H.; Liu, J.Y.; Huang, E.S.; Karter, A.J. The Legacy Effect in Type 2 Diabetes: Impact of Early Glycemic Control on Future Complications (The Diabetes & Aging Study). *Diabetes Care* **2019**, *42*, 416–426.
9. Moodahadu, L.S.; Dhall, R.; Zargar, A.H.; Bangera, S.; Ramani, L.; Katipally, R. Tight Glycemic Control and Cardiovascular Effects in Type 2 Diabetic Patients. *Heart Views* **2014**, *15*, 111–120. [\[CrossRef\]](#)
10. Hill, D.; Fisher, M. The effect of intensive glycaemic control on cardiovascular outcomes. *Diabetes Obes. Metab.* **2010**, *12*, 641–647. [\[CrossRef\]](#)
11. Punthakee, Z.; Miller, M.E.; Simmons, D.L.; Riddle, M.C.; Ismail-Beigi, F.; Brillon, D.J.; Bergenstal, R.M.; Savage, P.J.; Hramiak, I.; Largay, J.F.; et al. Durable change in glycaemic control following intensive management of type 2 diabetes in the ACCORD clinical trial. *Diabetologia* **2014**, *57*, 2030–2037. [\[CrossRef\]](#)
12. Bousageon, R.; Bejan-Angoulvant, T.; Saadatian-Elahi, M.; Lafont, S.; Bergeonneau, C.; Kassai, B.; Erpeldinger, S.; Wright, J.M.; Gueyffier, F.; Cornu, C. Effect of intensive glucose lowering treatment on all cause mortality, cardiovascular death, and microvascular events in type 2 diabetes: Meta-analysis of randomised controlled trials. *BMJ* **2011**, *343*, d4169. [\[CrossRef\]](#)
13. ADVANCE Collaborative Group; Patel, A.; MacMahon, S.; Chalmers, J.; Neal, B.; Billot, L.; Woodward, M.; Marre, M.; Cooper, M.; Glasziou, P.; et al. Intensive blood glucose control and vascular outcomes in patients with type 2 diabetes. *N. Engl. J. Med.* **2008**, *358*, 2560–2572. [\[CrossRef\]](#)
14. Donath, M.Y.; Shoelson, S.E. Type 2 diabetes as an inflammatory disease. *Nat. Rev. Immunol.* **2011**, *11*, 98–107. [\[CrossRef\]](#)
15. Lontchi-Yimagou, E.; Sobngwi, E.; Matsha, T.E.; Kengne, A.P. Diabetes mellitus and inflammation. *Curr. Diabetes Rep.* **2013**, *13*, 435–444. [\[CrossRef\]](#)
16. Cruz, N.G.; Sousa, L.P.; Sousa, M.O.; Pietrani, N.T.; Fernandes, A.P.; Gomes, K.B. The linkage between inflammation and Type 2 diabetes mellitus. *Diabetes Res. Clin. Pract.* **2013**, *99*, 85–92. [\[CrossRef\]](#)
17. Valentine, W.; Palmer, A.; Nicklasson, L.; Cobden, D.; Roze, S. Improving life expectancy and decreasing the incidence of complications associated with type 2 diabetes: A modelling study of HbA1c targets. *Int. J. Clin. Pract.* **2006**, *60*, 1138–1145. [\[CrossRef\]](#)
18. Lainampetch, J.; Panprathip, P.; Phosat, C.; Chumpathat, N.; Prangthip, P.; Soonthornworasiri, N.; Puduang, S.; Wechjakwen, N.; Kwanbunjan, K. Association of Tumor Necrosis Factor Alpha, Interleukin 6, and C-Reactive Protein with the Risk of Developing Type 2 Diabetes: A Retrospective Cohort Study of Rural Thais. *J. Diabetes Res.* **2019**, *2019*, 9051929. [\[CrossRef\]](#)
19. Fadaei, R.; Bagheri, N.; Heidarian, E.; Nouri, A.; Hesari, Z.; Moradi, N.; Ahmadi, A.; Ahmadi, R. Serum levels of IL-32 in patients with type 2 diabetes mellitus and its relationship with TNF- α and IL-6. *Cytokine* **2020**, *125*, 154832. [\[CrossRef\]](#)
20. Donath, M.Y.; Dinarello, C.A.; Mandrup-Poulsen, T. Targeting innate immune mediators in type 1 and type 2 diabetes. *Nat. Rev. Immunol.* **2019**, *19*, 734–746. [\[CrossRef\]](#)
21. Burgos-Morón, E.; Abad-Jiménez, Z.; De Marañón, A.M.; Iannantuoni, F.; Escribano-López, I.; López-Domènech, S.; Salom, C.; Jover, A.; Llabata, V.; Torres, I.R.; et al. Relationship between Oxidative Stress, ER Stress, and Inflammation in Type 2 Diabetes: The Battle Continues. *J. Clin. Med.* **2019**, *8*, 1385. [\[CrossRef\]](#)
22. Forrester, S.J.; Kikuchi, D.S.; Hernandez, M.S.; Xu, Q.; Griendling, K.K. Reactive Oxygen Species in Metabolic and Inflammatory Signaling. *Circ. Res.* **2018**, *122*, 877–902. [\[CrossRef\]](#)
23. Zhou, R.; Yazdi, A.S.; Menu, P.; Tschopp, J. A role for mitochondria in NLRP3 inflammasome activation. *Nature* **2011**, *469*, 221–225. [\[CrossRef\]](#)
24. Bulua, A.C.; Simon, A.; Maddipati, R.; Pelletier, M.; Park, H.; Kim, K.-Y.; Sack, M.N.; Kastner, D.L.; Siegel, R.M. Mitochondrial reactive oxygen species promote production of proinflammatory cytokines and are elevated in TNFR1-associated periodic syndrome (TRAPS). *J. Exp. Med.* **2011**, *208*, 519–533. [\[CrossRef\]](#)

25. Ungvari, Z.; Orosz, Z.; Labinsky, N.; Rivera, A.; Xiangmin, Z.; Smith, K.; Csiszar, A. Increased mitochondrial H₂O₂ production promotes endothelial NF- κ B activation in aged rat arteries. *Am. J. Physiol. Heart Circ. Physiol.* **2007**, *293*, H37–H47. [[CrossRef](#)]
26. Shah, A.; Xia, L.; Goldberg, H.; Lee, K.W.; Quaggin, S.E.; Fantus, I.G. Thioredoxin-interacting protein mediates high glucose-induced reactive oxygen species generation by mitochondria and the NADPH oxidase, Nox4, in mesangial cells. *J. Biol. Chem.* **2013**, *288*, 6835–6848. [[CrossRef](#)]
27. Zhou, R.; Tardivel, A.; Thorens, B.; Choi, I.; Tschopp, J. Thioredoxin-interacting protein links oxidative stress to inflammasome activation. *Nat. Immunol.* **2010**, *11*, 136–140. [[CrossRef](#)]
28. Yang, B.; Fritsche, K.L.; Beversdorf, D.Q.; Gu, Z.; Lee, J.C.; Folk, W.R.; Greenleaf, C.M.; Sun, G.Y. Yin-Yang Mechanisms Regulating Lipid Peroxidation of Docosahexaenoic Acid and Arachidonic Acid in the Central Nervous System. *Front. Neurol.* **2019**, *10*, 642. [[CrossRef](#)]
29. Fischer, R.; Maier, O. Interrelation of Oxidative Stress and Inflammation in Neurodegenerative Disease: Role of TNF. *Oxid. Med. Cell. Longev.* **2015**, *2015*, 610813. [[CrossRef](#)]
30. Guo, Y.; Zhuang, X.; Huang, Z.; Zou, J.; Yang, D.; Hu, X.; Du, Z.; Wang, L.; Liao, X. Klotho protects the heart from hyperglycemia-induced injury by inactivating ROS and NF- κ B-mediated inflammation both in vitro and in vivo. *Biochim. Biophys. Acta Mol. Basis Dis.* **2018**, *1864*, 238–251. [[CrossRef](#)]
31. Luo, B.; Li, B.; Wang, W.; Liu, X.; Xia, Y.; Zhang, C.; Zhang, M.; Zhang, Y.; An, F. NLRP3 gene silencing ameliorates diabetic cardiomyopathy in a type 2 diabetes rat model. *PLoS ONE* **2014**, *9*, e104771. [[CrossRef](#)]
32. Zhang, H.-L.; Chen, X.; Zong, B.; Yuan, H.; Wang, Z.; Wei, Y.; Wang, X.; Liu, G.; Zhang, J.; Li, S.; et al. Gypenosides improve diabetic cardiomyopathy by inhibiting ROS-mediated NLRP3 inflammasome activation. *J. Cell. Mol. Med.* **2018**, *22*, 4437–4448. [[CrossRef](#)]
33. Le Rossignol, S.; Ketheesan, N.; Haleagrahara, N. Redox-sensitive transcription factors play a significant role in the development of rheumatoid arthritis. *Int. Rev. Immunol.* **2018**, *37*, 129–143. [[CrossRef](#)]
34. Lepetsos, P.; Papavassiliou, K.A.; Papavassiliou, A.G. Redox and NF- κ B signaling in osteoarthritis. *Free Radic. Biol. Med.* **2019**, *132*, 90–100. [[CrossRef](#)]
35. Pradhan, A.; Bagchi, A.; De, S.; Mitra, S.; Mukherjee, S.; Ghosh, P.; Ghosh, A.; Chatterjee, M. Role of redox imbalance and cytokines in mediating oxidative damage and disease progression of patients with rheumatoid arthritis. *Free Radic. Res.* **2019**, *53*, 768–779. [[CrossRef](#)]
36. Duecker, R.; Baer, P.C.; Eickmeier, O.; Strecker, M.; Kurz, J.; Schaible, A.; Henrich, D.; Zielen, S.; Schubert, R. Oxidative stress-driven pulmonary inflammation and fibrosis in a mouse model of human ataxia-telangiectasia. *Redox Biol.* **2018**, *14*, 645–655. [[CrossRef](#)]
37. Nandi, A.; Bishayi, B. CCR-2 neutralization augments murine fresh BMC activation by *Staphylococcus aureus* via two distinct mechanisms: At the level of ROS production and cytokine response. *Innate Immun.* **2017**, *23*, 345–372. [[CrossRef](#)]
38. Diehl, A.M. Cytokine regulation of liver injury and repair. *Immunol. Rev.* **2000**, *174*, 160–171. [[CrossRef](#)]
39. Han, S.; Cai, W.; Yang, X.; Jia, Y.; Zheng, Z.; Wang, H.; Li, J.; Li, Y.; Gao, J.; Fan, L.; et al. ROS-Mediated NLRP3 Inflammasome Activity Is Essential for Burn-Induced Acute Lung Injury. *Mediat. Inflamm.* **2015**, *2015*, 720457. [[CrossRef](#)]
40. Lee, I.-T.; Yang, C.-M. Role of NADPH oxidase/ROS in pro-inflammatory mediators-induced airway and pulmonary diseases. *Biochem. Pharmacol.* **2012**, *84*, 581–590. [[CrossRef](#)]
41. Zuo, L.; Prather, E.R.; Stetskiv, M.; Garrison, D.E.; Meade, J.R.; Peace, T.I.; Zhou, T. Inflammaging and Oxidative Stress in Human Diseases: From Molecular Mechanisms to Novel Treatments. *Int. J. Mol. Sci.* **2019**, *20*, 4472. [[CrossRef](#)]
42. Ouedraogo, R.; Gong, Y.; Berzins, B.; Wu, X.; Mahadev, K.; Hough, K.; Chan, L.; Goldstein, B.J.; Scalia, R. Adiponectin deficiency increases leukocyte-endothelium interactions via upregulation of endothelial cell adhesion molecules in vivo. *J. Clin. Investig.* **2007**, *117*, 1718–1726. [[CrossRef](#)]
43. Yan, Y.; Li, S.; Liu, Y.; Bazzano, L.; He, J.; Mi, J.; Chen, W. Temporal relationship between inflammation and insulin resistance and their joint effect on hyperglycemia: The Bogalusa Heart Study. *Cardiovasc. Diabetol.* **2019**, *18*, 109. [[CrossRef](#)]
44. Galkina, E.; Ley, K. Immune and Inflammatory Mechanisms of Atherosclerosis. *Annu. Rev. Immunol.* **2009**, *27*, 165–197. [[CrossRef](#)]
45. Legein, B.; Temmerman, L.; Biessen, E.A.L.; Lutgens, E. Inflammation and immune system interactions in atherosclerosis. *Cell. Mol. Life Sci.* **2013**, *70*, 3847–3869. [[CrossRef](#)]

46. Kavousi, M.; Elias-Smale, S.; Rutten, J.H.; Leening, M.J.G.; Vliegenthart, R.; Verwoert, G.C.; Krestin, G.P.; Oudkerk, M.; De Maat, M.P.; Leebeek, F.W.; et al. Evaluation of newer risk markers for coronary heart disease risk classification: A cohort study. *Ann. Intern. Med.* **2012**, *156*, 438–444. [[CrossRef](#)]
47. Lau, K.K.; Wong, Y.-K.; Chan, Y.-H.; Yiu, K.-H.; Teo, K.C.; Li, L.S.-W.; Ho, S.-L.; Chan, K.H.; Siu, C.-W.; Tse, H.-F. Prognostic implications of surrogate markers of atherosclerosis in low to intermediate risk patients with type 2 diabetes. *Cardiovasc. Diabetol.* **2012**, *11*, 101. [[CrossRef](#)]
48. Ortega, E.; Gilabert, R.; Núñez, I.; Cofán, M.; Sala-Vila, A.; De Groot, E.; Ros, E. White blood cell count is associated with carotid and femoral atherosclerosis. *Atherosclerosis* **2012**, *221*, 275–281. [[CrossRef](#)]
49. Blüher, M.; Unger, R.; Rassoul, F.; Richter, V.; Paschke, R. Relation between glycaemic control, hyperinsulinaemia and plasma concentrations of soluble adhesion molecules in patients with impaired glucose tolerance or Type II diabetes. *Diabetologia* **2002**, *45*, 210–216. [[CrossRef](#)]
50. Jude, E.B.; Douglas, J.T.; Anderson, S.G.; Young, M.J.; Boulton, A.J.M. Circulating cellular adhesion molecules ICAM-1, VCAM-1, P- and E-selectin in the prediction of cardiovascular disease in diabetes mellitus. *Eur. J. Intern. Med.* **2002**, *13*, 185–189. [[CrossRef](#)]
51. Pankow, J.S.; Decker, P.A.; Berardi, C.; Hanson, N.Q.; Sale, M.; Tang, W.; Kanaya, A.M.; Larson, N.B.; Tsai, M.; Wassel, C.L.; et al. Circulating cellular adhesion molecules and risk of diabetes: The Multi-Ethnic Study of Atherosclerosis (MESA). *Diabet. Med.* **2016**, *33*, 985–991. [[CrossRef](#)]
52. Qiu, S.; Cai, X.; Liu, J.; Yang, B.; Zügel, M.; Steinacker, J.M.; Sun, Z.; Schumann, U. Association between circulating cell adhesion molecules and risk of type 2 diabetes: A meta-analysis. *Atherosclerosis* **2019**, *287*, 147–154. [[CrossRef](#)]
53. Nguyen, P.A.; Won, J.S.; Rahman, M.K.; Bae, E.J.; Cho, M.K. Modulation of Sirt1/NF- κ B interaction of evogliptin is attributed to inhibition of vascular inflammatory response leading to attenuation of atherosclerotic plaque formation. *Biochem. Pharmacol.* **2019**, *168*, 452–464. [[CrossRef](#)]
54. Sardu, C.; De Lucia, C.; Wallner, M.; Santulli, G. Diabetes Mellitus and Its Cardiovascular Complications: New Insights into an Old Disease. *J. Diabetes Res.* **2019**, *2019*, 1905194. [[CrossRef](#)]
55. Rangel, É.B.; Rodrigues, C.O.; de Sá, J.R. Micro- and Macrovascular Complications in Diabetes Mellitus: Preclinical and Clinical Studies. *J. Diabetes Res.* **2019**, *2019*, 2161085. [[CrossRef](#)]
56. Golden, S.H.; Folsom, A.R.; Coresh, J.; Sharrett, A.R.; Szklo, M.; Brancati, F. Risk factor groupings related to insulin resistance and their synergistic effects on subclinical atherosclerosis: The atherosclerosis risk in communities study. *Diabetes* **2002**, *51*, 3069–3076. [[CrossRef](#)]
57. Tabatabaei-Malazy, O.; Fakhrzadeh, H.; Sharifi, F.; Mirarefin, M.; Arzaghi, S.M.; Badamchizadeh, Z.; Alizadeh-Khoei, M.; Larijani, B. Effect of metabolic control on oxidative stress, subclinical atherosclerosis and peripheral artery disease in diabetic patients. *J. Diabetes Metab. Disord.* **2015**, *14*, 84. [[CrossRef](#)]
58. Alharby, H.; Abdelati, T.; Rizk, M.; Youssef, E.; Moghazy, K.; Gaber, N.; Yafei, S. Association of lipid peroxidation and interleukin-6 with carotid atherosclerosis in type 2 diabetes. *Cardiovasc. Endocrinol. Metab.* **2019**, *8*, 73–76. [[CrossRef](#)]
59. Bauer, M.; Caviezel, S.; Teynor, A.; Erbel, R.; Mahabadi, A.A.; Schmidt-Trucksäss, A. Carotid intima-media thickness as a biomarker of subclinical atherosclerosis. *Swiss Med. Wkly.* **2012**, *142*, w13705. [[CrossRef](#)]
60. Abd El Dayem, S.M.; Battah, A.A.; El Bohy, A.E.M. Assessment of Increase in Aortic and Carotid Intimal Medial Thickness in Type 1 Diabetic Patients. *Open Access Maced. J. Med. Sci.* **2016**, *4*, 630. [[CrossRef](#)]
61. Pignoli, P.; Tremoli, E.; Poli, A.; Oreste, P.; Paoletti, R. Intimal plus medial thickness of the arterial wall: A direct measurement with ultrasound imaging. *Circulation* **1986**, *74*, 1399–1406. [[CrossRef](#)]
62. Santos, I.S.; Bittencourt, M.S.; Goulart, A.C.; Schmidt, M.I.; Diniz, M.D.F.H.S.; Lotufo, P.A.; Benseñor, I.M. Insulin resistance is associated with carotid intima-media thickness in non-diabetic subjects. A cross-sectional analysis of the ELSA-Brasil cohort baseline. *Atherosclerosis* **2017**, *260*, 34–40. [[CrossRef](#)]
63. Jeevarethinam, A.; Venuraju, S.; Dumo, A.; Ruano, S.; Mehta, V.S.; Rosenthal, M.; Nair, D.; Cohen, M.; Darko, D.; Lahiri, A.; et al. Relationship between carotid atherosclerosis and coronary artery calcification in asymptomatic diabetic patients: A prospective multicenter study. *Clin. Cardiol.* **2017**, *40*, 752–758. [[CrossRef](#)] [[PubMed](#)]
64. O’Leary, D.H.; Polak, J.F.; Kronmal, R.A.; Manolio, T.A.; Burke, G.L.; Wolfson, S.K. Carotid-Artery Intima and Media Thickness as a Risk Factor for Myocardial Infarction and Stroke in Older Adults. *N. Engl. J. Med.* **1999**, *340*, 14–22. [[CrossRef](#)] [[PubMed](#)]

65. Lorenz, M.W.; Price, J.F.; Robertson, C.; Bots, M.L.; Polak, J.F.; Poppert, H.; Kavousi, M.; Dorr, M.; Stensland, E.; Ducimetiere, P.; et al. Carotid intima-media thickness progression and risk of vascular events in people with diabetes: Results from the PROG-IMT collaboration. *Diabetes Care* **2015**, *38*, 1921–1929. [[CrossRef](#)] [[PubMed](#)]
66. Tenjin, A.; Nagai, Y.; Yuji, S.; Ishii, S.; Kato, H.; Ohta, A.; Tanaka, Y. Short-term change of carotid intima-media thickness after treatment of hyperglycemia in patients with diabetes: A cross-sectional study. *BMC Res. Notes* **2016**, *9*, 281. [[CrossRef](#)]
67. Asemi, Z.; Raygan, F.; Bahmani, F.; Rezavandi, Z.; Talari, H.R.; Rafiee, M.; Poladchang, S.; Mofrad, M.D.; Taheri, S.; Mohammadi, A.A.; et al. The effects of vitamin D, K and calcium co-supplementation on carotid intima-media thickness and metabolic status in overweight type 2 diabetic patients with CHD. *Br. J. Nutr.* **2016**, *116*, 286–293. [[CrossRef](#)]
68. Herder, M.; Arntzen, K.; Johnsen, S.; Mathiesen, E. The metabolic syndrome and progression of carotid atherosclerosis over 13 years. The Tromsø Study. *Cardiovasc. Diabetol.* **2012**, *11*, 77. [[CrossRef](#)]
69. Escribano-López, I.; De Marañón, A.M.; Iannantuoni, F.; López-Domènech, S.; Abad-Jiménez, Z.; Díaz-Pozo, P.; Sola, E.; Apostolova, N.; Rocha, M.; Víctor, V.M. The Mitochondrial Antioxidant SS-31 Modulates Oxidative Stress, Endoplasmic Reticulum Stress, and Autophagy in Type 2 Diabetes. *J. Clin. Med.* **2019**, *8*, 1322. [[CrossRef](#)]
70. González, F.; Rote, N.S.; Minium, J.; Kirwan, J.P. Reactive oxygen species-induced oxidative stress in the development of insulin resistance and hyperandrogenism in polycystic ovary syndrome. *J. Clin. Endocrinol. Metab.* **2006**, *91*, 336–340. [[CrossRef](#)]
71. Bajpai, A.; Tilley, D.G. The Role of Leukocytes in Diabetic Cardiomyopathy. *Front. Physiol.* **2018**, *9*, 1547. [[CrossRef](#)] [[PubMed](#)]
72. Mijares, A.H.; Rocha, M.; Rovira-Llopis, S.; Bañuls, C.; Bellod, L.; De Pablo, C.; Alvarez, A.; Roldán, I.; Sola-Izquierdo, E.; Victor, V.M. Human Leukocyte/Endothelial Cell Interactions and Mitochondrial Dysfunction in Type 2 Diabetic Patients and Their Association with Silent Myocardial Ischemia. *Diabetes Care* **2013**, *36*, 1695–1702. [[CrossRef](#)]
73. Alcántar-Fernández, J.; González-Maciel, A.; Reynoso-Robles, R.; Andrade, M.E.P.; Hernández-Vázquez, A.D.J.; Velázquez-Arellano, A.; Miranda-Ríos, J. High-glucose diets induce mitochondrial dysfunction in *Caenorhabditis elegans*. *PLoS ONE* **2019**, *14*, e0226652. [[CrossRef](#)]
74. Lin, H.-Y.; Weng, S.-W.; Chang, Y.-H.; Su, B.Y.-J.; Chang, C.-M.; Tsai, C.-J.; Shen, F.-C.; Chuang, J.-H.; Lin, T.-K.; Liou, C.-W.; et al. The Causal Role of Mitochondrial Dynamics in Regulating Insulin Resistance in Diabetes: Link through Mitochondrial Reactive Oxygen Species. *Oxid. Med. Cell. Longev.* **2018**, *2018*, 7514383. [[CrossRef](#)]
75. Rehman, K.; Akash, M.S.H. Mechanism of Generation of Oxidative Stress and Pathophysiology of Type 2 Diabetes Mellitus: How Are They Interlinked? *J. Cell. Biochem.* **2017**, *118*, 3577–3585. [[CrossRef](#)]
76. Luc, K.; Schramm-Luc, A.; Guzik, T.J.; Mikolajczyk, T.P. Oxidative stress and inflammatory markers in prediabetes and diabetes. *J. Physiol. Pharmacol.* **2019**, *70*, 809–824.
77. Diao, F.-Y.; Xu, M.; Hu, Y.; Li, J.; Xu, Z.; Lin, M.; Wang, L.; Zhou, Y.; Zhou, Z.; Liu, J.; et al. The molecular characteristics of polycystic ovary syndrome (PCOS) ovary defined by human ovary cDNA microarray. *J. Mol. Endocrinol.* **2004**, *33*, 59–72. [[CrossRef](#)]
78. Dupré-Crochet, S.; Erard, M.; Nüße, O. ROS production in phagocytes: Why, when, and where? *J. Leukoc. Biol.* **2013**, *94*, 657–670. [[CrossRef](#)]
79. Rao, K.M.K. MAP kinase activation in macrophages. *J. Leukoc. Biol.* **2001**, *69*, 3–10.
80. Okazaki, S.; Sakaguchi, M.; Miwa, K.; Furukado, S.; Yamagami, H.; Yagita, Y.; Mochizuki, H.; Kitagawa, K. Association of interleukin-6 with the progression of carotid atherosclerosis: A 9-year follow-up study. *Stroke* **2014**, *45*, 2924–2929. [[CrossRef](#)]
81. Skoog, T.; Dichl, W.; Boquist, S.; Skoglund-Andersson, C.; Karpe, F.; Tang, R.; Bond, M.; De Faire, U.; Nilsson, J.; Eriksson, P.; et al. Plasma tumour necrosis factor-alpha and early carotid atherosclerosis in healthy middle-aged men. *Eur. Heart J.* **2002**, *23*, 376–383. [[CrossRef](#)]
82. Ijsselmuiden, A.J.; Musters, R.J.; De Ruiter, G.; Van Heerebeek, L.; Alderse-Baas, F.; Van Schilfgaarde, M.; Leyte, A.; Tangelder, G.-J.; Laarman, G.J.; Paulus, W.J. Circulating white blood cells and platelets amplify oxidative stress in heart failure. *Nat. Clin. Pract. Cardiovasc. Med.* **2008**, *5*, 811–820. [[CrossRef](#)]

83. Bárány, T.; Simon, A.; Szabó, G.; Benkő, R.; Mezei, Z.; Molnár, L.; Becker, D.; Merkely, B.; Zima, E.; Horváth, E.M. Oxidative Stress-Related Parthanatos of Circulating Mononuclear Leukocytes in Heart Failure. *Oxid. Med. Cell. Longev.* **2017**, *2017*, 1249614. [[CrossRef](#)]
84. Tiyerili, V.; Camara, B.; Becher, M.U.; Schrickel, J.W.; Lütjohann, D.; Mollenhauer, M.; Baldus, S.; Nickenig, G.; Andrié, R.P. Neutrophil-derived myeloperoxidase promotes atherogenesis and neointima formation in mice. *Int. J. Cardiol.* **2016**, *204*, 29–36. [[CrossRef](#)]
85. Victor, V.M.; Rocha, M.; Sola, E.; Banuls, C.; Garcia-Malpartida, K.; Hernandez-Mijares, A. Oxidative Stress, Endothelial Dysfunction and Atherosclerosis. *Curr. Pharm. Des.* **2009**, *15*, 2988–3002. [[CrossRef](#)]
86. Pettersson, U.S.; Christoffersson, G.; Massena, S.; Ahl, D.; Jansson, L.; Henriksnäs, J.; Phillipson, M. Increased Recruitment but Impaired Function of Leukocytes during Inflammation in Mouse Models of Type 1 and Type 2 Diabetes. *PLoS ONE* **2011**, *6*, e22480. [[CrossRef](#)]
87. Novak, V.; Zhao, P.; Manor, B.; Sejdíć, E.; Alsop, D.; Abduljalil, A.; Roberson, P.K.; Munshi, M.; Novak, P. Adhesion molecules, altered vasoreactivity, and brain atrophy in type 2 diabetes. *Diabetes Care* **2011**, *34*, 2438–2441. [[CrossRef](#)]
88. Giugliano, D.; Marfella, R.; Coppola, L.; Verrazzo, G.; Acampora, R.; Giunta, R.; Nappo, F.; Lucarelli, C.; D’Onofrio, F. Vascular Effects of Acute Hyperglycemia in Humans Are Reversed by L-Arginine. *Circulation* **1997**, *95*, 1783–1790. [[CrossRef](#)]
89. Kolluru, G.K.; Bir, S.C.; Kevil, C.G. Endothelial dysfunction and diabetes: Effects on angiogenesis, vascular remodeling, and wound healing. *Int. J. Vasc. Med.* **2012**, *2012*, 918267. [[CrossRef](#)]
90. Nezu, T.; Hosomi, N.; Aoki, S.; Matsumoto, M. Carotid Intima-Media Thickness for Atherosclerosis. *J. Atheroscler. Thromb.* **2016**, *23*, 18–31. [[CrossRef](#)]
91. Zhao, B.; Liu, Y.; Zhang, Y.; Chen, Y.; Yang, Z.-F.; Zhu, Y.; Xu, S. Gender difference in carotid intima-media thickness in type 2 diabetic patients: A 4-year follow-up study. *Cardiovasc. Diabetol.* **2012**, *11*, 51. [[CrossRef](#)]
92. Luo, X.; Yang, Y.; Cao, T.; Li, Z. Differences in left and right carotid intima-media thickness and the associated risk factors. *Clin. Radiol.* **2011**, *66*, 393–398. [[CrossRef](#)]
93. Hedna, V.S.; Bodhit, A.N.; Ansari, S.; Falchook, A.D.; Stead, L.; Heilman, K.M.; Waters, M.F. Hemispheric Differences in Ischemic Stroke: Is Left-Hemisphere Stroke More Common? *J. Clin. Neurol.* **2013**, *9*, 97–102. [[CrossRef](#)]
94. Hernaández, S.A.R.; Kroon, A.A.; Van Boxtel, M.P.; Mess, W.H.; Lodder, J.; Jolles, J.; De Leeuw, P.W. Is there a side predilection for cerebrovascular disease? *Hypertension* **2003**, *42*, 56–60. [[CrossRef](#)]
95. Selwaness, M.; Bouwhuisen, Q.V.D.; Van Onkelen, R.S.; Hofman, A.; Franco, O.H.; Van Der Lugt, A.; Wentzel, J.J.; Vernooij, M.W. Atherosclerotic plaque in the left carotid artery is more vulnerable than in the right. *Stroke* **2014**, *45*, 3226–3230. [[CrossRef](#)]
96. Einarson, T.R.; Hunchuck, J.; Hemels, M. Relationship between blood glucose and carotid intima media thickness: A meta-analysis. *Cardiovasc. Diabetol.* **2010**, *9*, 37. [[CrossRef](#)]
97. Pillai, P.R.; Tiwari, D.; Jatav, O.P.; Rai, H. Lipid profile and carotid artery intima-media thickness in diabetic and non-diabetic ischaemic stroke. *Int. J. Adv. Med.* **2017**, *4*, 471. [[CrossRef](#)]

